Advanced Structural Mechanics 1 (2023) 81-101

Advanced Structural Mechanics

journal homepage: http://asm.sku.ac.ir

Free vibration analysis of viscoelastic nano-sandwich beam with flexible core resting on orthotropic Pasternak medium using non local high order sandwich panel theory

Mohsen Botshekanan Dehkordi[a*], Ali Cheraghbak[b]

[a]*Faculty of Engineering, Shahrekourd University, Shahrekord, Iran*

[b]*Faculty of Engineering, Shahrekourd University, Shahrekord, Iran*

Article received: 2022/11/13, Article revised: 2023/01/20, Article accepted: 2023/01/20

ABSTRACT

In this paper, vibration analysis of nonlocal nano-sandwich beam is investigated considering the size effects and flexibility of the core. This nano-sandwich beam is made from double beam and a flexible core. In the analytical formulation, normal and shear stresses are considered for the core employing the high order sandwich panel theory. In this regard the high order sandwich panel theory is extended at nano-scale. The material properties of system are assumed viscoelastic using Kelvin–Voigt model. The elastic medium is simulated by orthotropic Pasternak medium. The final equations are governed by Hamilton's principle. The Navier method is applied for obtaining the natural frequency response of nano sandwich beam. The effects of different parameters such as nonlocal parameter, structural damping, viscoelastic foundation, geometrical parameters and stiffness of the core are shown on the vibration behavior of nanostructure. The accuracy of the proposed method is verified by comparing its numerical predictions with other published works. The results show that with increasing the nonlocal parameter, the frequency decreases.

Keywords: Free vibration, Nano sandwich beam, flexible core, high order sandwich panel theory, Size effect

1. Introduction

Sandwich structures have much application in different industries due to the high hardness-to-weight and strength-to-weight ratios and other better properties compared with traditional isotropic ones. These structures can be used in aircraft, helicopters, missiles, launchers, satellites etc. During the last five decades the application of sandwich structures with light core and two thin factsheets have been extensively investigated.

* Corresponding author at: Faculty of Engineering, Shahrekord University, Shahrekord, Iran.
E-mail address: botshekanan@sku.ac.ir.

DOI: 10.22034/asm.2023.14145.1008: http://asm.sku.ac.ir/article_11383.html

Mechanical analysis of macro sandwich structures has been studied by many researchers. A simple isoparametric assumed-strain finite element formulation incorporating a third-order polynomial displacement model for the buckling and vibration analysis of initially stressed composite sandwich laminates was presented by Nayak et al. [1]. Analytical models with geometric non-linearities accounting for interactions between local and global instability modes leading to localized buckling in sandwich struts were formulated by Ahmer Wadee et al. [2]. El Meiche et al., [3] considered a new hyperbolic shear deformation theory taking into account transverse shear deformation effects for the buckling and free vibration analysis of thick functionally graded sandwich plates. Rohlfing et al., [4] presented an experimental work to compare the effect of decentralized velocity feedback control on thin homogeneous and sandwich panels. Ghayesh [5] investigated the forced dynamics of an axially moving viscoelastic beam. Liu et al., [6] studied dynamic responses of axially moving viscoelastic beam subject to a randomly disordered periodic excitation. Ghayesh and Amabili [7] analyzed the nonlinear forced dynamics of an axially moving viscoelastic beam in the supercritical speed regime, when the system was beyond the first instability order. Influence of viscoelastic and auxetic (Negative Poisson's Ratio NPR) layers on the free vibration modeling of a composite sandwich structure was analyzed by Azoti et al. [8]. The analytical, numerical and experimental study of the bifurcation and collapse behavior of a 3D reinforced sandwich structure under through- thickness compression was conducted by Laine et al. [9]. Kueh [10] investigated computationally the buckling of simply supported sandwich columns constructed using elastic cores reinforced by skin-sheets of triaxle weave fabric composites. Teodor et al. [11] studied the forced oscillations of a rod with a body attached to its free end so that the motion of a system could be described by two sets of equations: integer and fractional. Non-linear dynamic response of a continuous sandwich beam with SMA hybrid composite face sheets and flexible core was analyzed by Khalili et al. [12]. El Mir et al. [13] presented the analysis of cylindrical sandwich structures with weak orthotropic core subjected to patch loading. Dynamic stability of a rotating three layered symmetric sandwich beam with magneto rheological elastomer core and conductive skins subjected to axial periodic loads was investigated by Nayak et al. [14]. Magnucka-Blandzi [15] studied the thin-walled simply supported sandwich beams: three and seven-layer beams. Stability of thin flexible Bernoulli-Euler beams was investigated by Krysko et al., [16] by considering the geometric non-linearity, as well as the type and intensity of the temperature field. Taking into account the phase transformation and material non-linearity effects for every point along the face sheets, Komijani and Gracie [17] examined dynamic characteristics of Functionally Graded Piezoelectric Material beams under in-plane and out-of-plane mechanical, thermal, and electrical excitations. Xiaobai Li et al., deduced a size-dependent inhomogeneous beam model, accounting for the through-length power-law variation of a two-constituent axially functionally graded material (FGM) [18].

None of the above works has reported the mechanical analysis of nano-sandwich structures. Chen et al. [19] investigated the dynamic stability of an axially accelerating viscoelastic beam undergoing parametric resonance. Static and dynamic buckling of an FGM beam subjected to uniform temperature rise loading and uniform compression were studied by Ghiasian et al [20]. Lei et al., [21] studied vibration of nonlocal Kelvin–Voigt viscoelastic damped Timoshenko beams. Eltaher et al., [22] investigated the static and buckling behaviors of nonlocal functionally graded (FG) Timoshenko nano beam. Ilkhani and Hashemi [23] studied the micro-electro-mechanical and nano-electro-mechanical machines such as micro/nano pumps that use a rotating beam as their energy transmission part. Behavior of beam-type micro/nano electromechanical systems (MEMSs/NEMSs) made of functionally graded sandwich materials subjected to electrostatic actuation effect and intermolecular Casimir forces was investigated by Shojaeian and Zeighampour. [24]. Bending and buckling of embedded nano-sandwich plates were investigated by Kolahchi [25] based on refined zigzag theory (RZT), sinusoidal shear deformation theory (SSDT), first order shear deformation theory (FSDT), and classical plate theory (CPT). Forced vibration of FG nano beams resting on the nonlinear elastic foundations was investigated by Tang et al. [26]. Arefi and Zenkour [27] studied thermo-electro-magneto-mechanical bending analysis of a sandwich nano plate based on the nonlocal strain gradient theory. Moreover, nonlinear amplitude-frequency response, unstable boundary and dynamic responses of an axially moving viscoelastic sandwich beam under low- and high-frequency principle resonances were discussed by Li et al. [28].

In this paper, vibration of sandwich nano-beam resting on orthotropic Pasternak medium is studied. The main novelty of this study is modeling of the sandwich beam with flexible core at nano scale considering the size effects using Eringen's theory and Kelvin-Voigt model to analysis the damping of structure. Moreover, the sandwich nano structure is made from upper beam, flexible core and lower beam. For modeling of beams and flexible core, the Euler–Bernoulli and the high order sandwich panel theories are used, respectively. For assuming the effect of small size and damping of structure, the Eringer theory and Kelvin–Voigt model are applied, respectively. Utilizing Hamilton's principle, the motion equations are obtained. Using Navier method, the frequency of the structure is obtained. The goal of this work is to investigate the effect of differed parameters such as, size effect, geometrical parameter, structure damping and Pasternak medium on the frequency of the sandwich nano-beam.

2. Formulation

A symmetric nano sandwich beam resting on elastic medium with length of L, thickness of core, and top and bottom face sheets receptivity is shown in Fig. 1.

2.1. Euler–Bernoulli

Based on Euler–Bernoulli beam model, the orthogonal components of the displacement vector can be written as:

$$\begin{aligned} u_i(x,z,t) &= u_{0i}(x,t) - z\frac{\partial w_{0i}(x,t)}{\partial x}, \qquad i=(t,b) \\ w_i(x,z,t) &= w_{0i}(x,t) \qquad\qquad\qquad\quad i=(t,b) \end{aligned} \tag{1}$$

where u_0 and w_0 is displacement in direction of length and thickness, respectively. However, the strain–displacement relations can be expressed as:

$$\begin{aligned} \varepsilon_{xx}^{t} &= \frac{\partial}{\partial x}u_{ot} - z_t\frac{\partial^2}{\partial x^2}w_b, \\ \varepsilon_{xx}^{b} &= \frac{\partial}{\partial x}u_{ob} - z_b\frac{\partial^2}{\partial x^2}w_b, \end{aligned} \tag{2}$$

Where the superscripts (t, b) are used to denote quantities corresponding to the upper and lower beams, respectively.

2.2. High order sandwich panel theory

Based on the high order sandwich panel theory, the displacement fields can be given as follows [29]:

$$\begin{aligned} w_c(z=0) &= u_{0t} - \frac{d_t}{2}w_{t,x}, \\ w_c(z=c) &= u_{0b} + \frac{d_b}{2}w_{b,x}, \end{aligned} \tag{3}$$

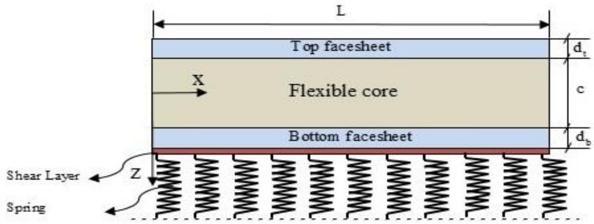

Fig. 1. A nano sandwich beam resting on elastic medium.

$$u_c = w_i, \tag{4}$$

where u_c , w_c is displacement in direction of length and thickness of the core, respectively. The kinematic unknown parameters of the high order sandwich panel theory are u_c and w_c , showing the axial and transverse core displacements, respectively. Hence, the strain-stress of this theory can be written as [25]:

$$\begin{aligned}
&\Big(1-\underset{\mu}{(e_0 a)}\nabla^2\Big)\sigma_{xxt}^{nl} = E_t\left(1+g\frac{\partial}{\partial t}\right)\varepsilon_{xxt},\\
&\Big(1-\underset{\mu}{(e_0 a)}\nabla^2\Big)\sigma_{xxb}^{nl} = E_b\left(1+g\frac{\partial}{\partial t}\right)\varepsilon_{xxb},
\end{aligned} \tag{5}$$

and for core we have:

$$\begin{aligned}
&\Big(1-\underset{\mu}{(e_0 a)}\nabla^2\Big)\tau^{nl} = G_c\left(1+g\frac{\partial}{\partial t}\right)\gamma,\\
&\Big(1-\underset{\mu}{(e_0 a)}\nabla^2\Big)\sigma_{zz}^{nl} = E_c\left(1+g\frac{\partial}{\partial t}\right)\frac{\partial}{\partial z}w_c,
\end{aligned} \tag{6}$$

where $\mu = e_0 a$ is small scale parameter; g is the structural damping parameter; E_t and E_b is Young's modulus of top and bottom face sheets, respectively; G_c and E_c is shear modulus and Young modulus of the core, respectively.

2.3 Motion equation

For driving the motion equations, the Hamilton's principle is used as follows:

$$\delta U - \delta W - \delta K = 0, \tag{7}$$

Where δ is variation, δU is variation of potential energy, δW is variation of kinematic energy and δK is variation of external work. The variation of potential energy for beams and flexible core can be written as:

$$\delta U = \int_{u_{top}} \sigma_{txx}^{nl}\delta\varepsilon_{xx}dv + \int_{u_{bot}} \sigma_{bxx}^{nl}\delta\varepsilon_{xx}dv + \int_{u_{core}} \tau_c^{nl}\delta\gamma_c dv + \int_{u_{core}} \sigma_{zz}^{nl}\delta\varepsilon_{zz}dv \tag{8}$$

The variation of kinematic energy can be given as follows:

$$\delta K = \int_{t_1}^{t_2}\left[\begin{aligned}&\int_0^L m_t\left(\dot{u}_{ot}\delta\dot{u}_{ot} + \dot{w}_t\delta\dot{w}_t\right)dx + \int_0^L m_b\left(\dot{u}_{ob}\delta\dot{u}_{ob} + \dot{w}_b\delta\dot{w}_b\right)dx\\ &+\int_{v_{core}} \rho_c\dot{u}_c\delta\dot{u}_c dv + \int_{v_{core}} \rho_c\dot{w}_c\delta\dot{w}_c dv\end{aligned}\right]dt, \tag{9}$$

where m_b and m_t is mass moment for the bottom and top beams, respectively, ρ_c is density core, $\dot{u}$ and $\dot{w}$ is derivative of time in directions of length and thickness, respectively.

The variation of external work, due to elastic medium load simulated by orthotropic Pasternak model can be expressed as [20]:

$$\delta W = \int \left(kg_1 \cos^2(\theta) \frac{\partial^2}{\partial x^2} w_b + kg_2 \sin^2(\theta) \frac{\partial^2}{\partial x^2} w_b - k_w w_b \right) dx, \tag{10}$$

where kg_1 and kg_2 is shear constant along 1 and 2 directions, respectively; θ is angel of shear layer with respect to 1 direction; k_w is spring constant.

2.4. Hamilton principle

Using Hamilton's principle and partial integral, the governing equations are computed as Eq. (11)

$$\begin{aligned} \delta u_{0t} : N^{nl}_{xxt,x} + \tau^{nl}_c (z=0) - m_t \frac{\partial^2}{\partial t^2} u_{0t} - \frac{m_c}{3} \frac{\partial^2}{\partial t^2} u_{0t} - \frac{m_c}{6} \frac{\partial^2}{\partial t^2} u_{0b} \\ + \frac{m_c d_t}{6} \frac{\partial^3}{\partial t^2 \partial x} w_t + \frac{m_c d_b}{12} \frac{\partial^3}{\partial t^2 \partial x} w_b + m_{1t} \frac{\partial^3}{\partial t^2 \partial x} w_t = 0, \end{aligned} \tag{11}$$

Equation (12):

$$\begin{aligned} \delta u_{0b} : N^{nl}_{xxb,x} + \tau^{nl}_c (z=0) - m_b \frac{\partial^2}{\partial t^2} u_{0t} - \frac{m_c}{6} \frac{\partial^2}{\partial t^2} u_{0t} - \frac{m_c}{3} \frac{\partial^2}{\partial t^2} u_{0b} \\ + \frac{m_c d_t}{12} \frac{\partial^3}{\partial t^2 \partial x} w_t - \frac{m_c d_b}{6} \frac{\partial^3}{\partial t^2 \partial x} w_b + m_{1b} \frac{\partial^3}{\partial t^2 \partial x} w_b = 0, \end{aligned} \tag{12}$$

Equation (13):

$$\begin{aligned} \delta w_t : M^{nl}_{xxt,xx} + \frac{d_t}{2} \tau^{nl}_{c,x} (z=c) + \sigma^{nl}_{zz} (z=0) - m_t \frac{\partial^2}{\partial t^2} w_t - \frac{m_c d_t}{6} \frac{\partial^3}{\partial t^2 \partial x} u_{0t} \\ - \frac{m_c d_b}{12} \frac{\partial^3}{\partial t^2 \partial x} u_{0b} + \frac{m_c d_t^2}{12} \frac{\partial^3}{\partial t^2 \partial x} w_t - \frac{m_c d_b d_t}{24} \frac{\partial^3}{\partial t^2 \partial x} w_b \\ - m_{1t} \frac{\partial^3}{\partial t^2 \partial x} u_{0t} + m_{2t} \frac{\partial^4}{\partial t^2 \partial x^2} w_t - \frac{m_c}{6} \frac{\partial^2}{\partial t^2} w_b - \frac{m_c}{3} \frac{\partial^2}{\partial t^2} w_t = 0, \end{aligned} \tag{13}$$

Equation (14):

$$\delta w_b : M^{nl}_{xxb,xx} + \frac{d_b}{2}\tau^{nl}_{c,x}(z=c) - \sigma^{nl}_{zz}(z=0) - m_b\frac{\partial^2}{\partial t^2}w_b + \frac{m_c d_b}{12}\frac{\partial^3}{\partial t^2\partial x}u_{0t}$$
$$+\frac{m_c d_b}{6}\frac{\partial^3}{\partial t^2\partial x}u_{0b} + \frac{m_c d_b^2}{12}\frac{\partial^3}{\partial t^2\partial x}w_b - \frac{m_c d_b d_t}{24}\frac{\partial^3}{\partial t^2\partial x}w_t - m_{1b}\frac{\partial^3}{\partial t^2\partial x}u_{0b}$$
$$+m_{2b}\frac{\partial^4}{\partial t^2\partial x^2}w_b - \frac{m_c}{6}\frac{\partial^2}{\partial t^2}w_t - \frac{m_c}{3}\frac{\partial^2}{\partial t^2}w_b - +kg_1\cos^2(\theta)\frac{\partial^2}{\partial x^2}w_b \tag{14}$$
$$+kg_2\, \mathrm{s}\,in^2(\theta)\frac{\partial^2}{\partial x^2}w_b - k_w w_b = 0,$$

Equation (15):

$$\delta w_c : \tau^{nl}_{c,x} + \sigma^{nl}_{zz,z} = 0, \tag{15}$$

Equation (16):

$$\delta u_c : \tau^{nl}_{c,x} = 0, \tag{16}$$

where the force and moment resultants can be defined as:

$$\left(1-\mu\nabla^2\right)N^{nl}_{txx} = N^{l}_{txx} = \int_{A^t}\sigma^{l}_{txx}dA = -E^t A_t\frac{\partial}{\partial x}u_{ot}, \tag{17}$$

$$\left(1-\mu\nabla^2\right)N^{nl}_{bxx} = N^{l}_{bxx} = \int_{A^t}\sigma^{l}_{bxx}dA = -E^b A_b\frac{\partial}{\partial x}u_{ob}, \tag{18}$$

$$\left(1-\mu\nabla^2\right)M^{nl}_{txx} = M^{l}_{txx} = \int_{A^t}\sigma^{l}_{txx}z\,dA = -E^t I_t\frac{\partial^2}{\partial x^2}w_t, \tag{19}$$

$$\left(1-\mu\nabla^2\right)M^{nl}_{bxx} = M^{l}_{bxx} = \int_{A^t}\sigma^{l}_{bxx}z\,dA = -E^b I_b\frac{\partial^2}{\partial x^2}w_b, \tag{20}$$

With solution of Eqs. (15) and (16) and applying compatibility conditions between the core and top face sheet, we have

$$u_c(x,z) = \frac{\tau^{nl}_c}{G_c}z + \frac{\tau^{nl}_{c,xx}}{2E_c}\left(\frac{z^3}{3} - c\frac{z^2}{2}\right) - w_{b,x}\frac{z^2}{2c} - w_{t,x}\left(z + \frac{d_t}{2} - \frac{z^2}{2c}\right) + u_{0t} \tag{21}$$
$$-\mu\frac{\partial^2}{\partial x^2}\left[\frac{\tau^{nl}_{c,xx}}{2E_c}\left(\frac{z^3}{3} - c\frac{z^2}{2}\right) + \frac{\tau^{nl}_c}{G_c}z\right],$$

$$w_c(x,z) = -\frac{\tau^{nl}_{c,x}}{2E_c}\left(z^2 - cz\right) + z\left(\frac{w_b - w_t}{c}\right) + w_t - \mu\frac{\partial^2}{\partial x^2}\left[-\frac{\tau^{nl}_{c,x}}{2E_c}\left(z^2 - cz\right)\right]. \tag{22}$$

Therefore, the governing equations of nano sandwich beam can be written as:

$$
\begin{aligned}
&-E^{t}A_{t}\left[\frac{\partial^2}{\partial x^2}u_{0t}+g.\frac{\partial^3}{\partial x^2\partial t}u_{0t}\right]+\tau b-m_t\frac{\partial^2}{\partial t^2}u_{0t}-\frac{m_c}{3}\frac{\partial^2}{\partial t^2}u_{0t}-\frac{m_c}{6}\frac{\partial^2}{\partial t^2}u_{0b}\\
&+\frac{m_c d_t}{6}\frac{\partial^3}{\partial t^2\partial x}w_t+\frac{m_c d_b}{12}\frac{\partial^3}{\partial t^2\partial x}w_b+m_{1t}\frac{\partial^3}{\partial t^2\partial x}w_t-\mu\frac{\partial^2}{\partial x^2}\left[\tau b-m_t\frac{\partial^2}{\partial t^2}u_{0t}-\frac{m_c}{3}\frac{\partial^2}{\partial t^2}u_{0t}\right.\\
&\left.-\frac{m_c}{6}\frac{\partial^2}{\partial t^2}u_{0b}+\frac{m_c d_t}{6}\frac{\partial^3}{\partial t^2\partial x}w_t+\frac{m_c d_b}{12}\frac{\partial^3}{\partial t^2\partial x}w_b+m_{1t}\frac{\partial^3}{\partial t^2\partial x}w_t\right]=0,
\end{aligned}
\tag{23}
$$

$$
\begin{aligned}
&-E^{b}A_{b}\left[\frac{\partial^2}{\partial x^2}u_{0b}+g.\frac{\partial^3}{\partial x^2\partial t}u_{0b}\right]-\tau-m_b\frac{\partial^2}{\partial t^2}u_{0t}-\frac{m_c}{6}\frac{\partial^2}{\partial t^2}u_{0t}-\frac{m_c}{3}\frac{\partial^2}{\partial t^2}u_{0b}\\
&+\frac{m_c d_t}{12}\frac{\partial^3}{\partial t^2\partial x}w_t-\frac{m_c d_b}{6}\frac{\partial^3}{\partial t^2\partial x}w_b+m_{1b}\frac{\partial^3}{\partial t^2\partial x}w_b-\mu\frac{\partial^2}{\partial x^2}\left[-\tau-m_b\frac{\partial^2}{\partial t^2}u_{0t}-\frac{m_c}{6}\frac{\partial^2}{\partial t^2}u_{0t}\right.\\
&\left.-\frac{m_c}{3}\frac{\partial^2}{\partial t^2}u_{0b}+\frac{m_c d_t}{12}\frac{\partial^3}{\partial t^2\partial x}w_t-\frac{m_c d_b}{6}\frac{\partial^3}{\partial t^2\partial x}w_b+m_{1b}\frac{\partial^3}{\partial t^2\partial x}w_b\right]=0,
\end{aligned}
\tag{24}
$$

$$
\begin{aligned}
&-E^{t}I_{t}\left[\frac{\partial^4}{\partial x^4}w_t+g.\frac{\partial^5}{\partial x^4\partial t}w_t\right]+\frac{bd_t\partial\tau}{2\partial x}+\left(\frac{E_c b(w_b-w_t)}{c}+\frac{gE_c b}{c}\left[\frac{\partial}{\partial t}w_b-\frac{\partial}{\partial t}w_t\right]+\frac{c}{2}\frac{\partial\tau}{\partial x}\right)b\\
&-m_t\frac{\partial^2}{\partial t^2}w_t-\frac{m_c d_t}{6}\frac{\partial^3}{\partial t^2\partial x}u_{0t}-\frac{m_c d_b}{12}\frac{\partial^3}{\partial t^2\partial x}u_{0b}+\frac{m_c d_t^2}{12}\frac{\partial^3}{\partial t^2\partial x}w_t-\frac{m_c d_b d_t}{24}\frac{\partial^3}{\partial t^2\partial x}w_b\\
&-m_{1t}\frac{\partial^3}{\partial t^2\partial x}u_{0t}+m_{2t}\frac{\partial^4}{\partial t^2\partial x^2}w_t-\frac{m_c}{6}\frac{\partial^2}{\partial t^2}w_b-\frac{m_c}{3}\frac{\partial^2}{\partial t^2}w_t-\mu\frac{\partial^2}{\partial x^2}\left[\frac{bd_t\partial\tau}{2\partial x}+\frac{c}{2}\frac{\partial\tau}{\partial x}b\right.\\
&+\frac{E_c b(w_b-w_t)}{c}+\frac{gE_c b}{c}\left[\frac{\partial}{\partial t}w_b-\frac{\partial}{\partial t}w_t\right]-m_t\frac{\partial^2}{\partial t^2}w_t-\frac{m_c d_t}{6}\frac{\partial^3}{\partial t^2\partial x}u_{0t}-\frac{m_c d_b}{12}\frac{\partial^3}{\partial t^2\partial x}u_{0b}\\
&\left.+\frac{m_c d_t^2}{12}\frac{\partial^3}{\partial t^2\partial x}w_t-\frac{m_c d_b d_t}{24}\frac{\partial^3}{\partial t^2\partial x}w_b-m_{1t}\frac{\partial^3}{\partial t^2\partial x}u_{0t}+m_{2t}\frac{\partial^4}{\partial t^2\partial x^2}w_t-\frac{m_c}{6}\frac{\partial^2}{\partial t^2}w_b-\frac{m_c}{3}\frac{\partial^2}{\partial t^2}w_t\right]=0,
\end{aligned}
\tag{25}
$$

$$-E^b I_b\left[\frac{\partial^4}{\partial x^4}w_b+g.\frac{\partial^5}{\partial x^4\partial t}w_b\right]+\frac{bd_b}{2}\frac{\partial\tau}{\partial x}-\left(\frac{E_c(w_b-w_t)}{c}+\frac{E_c g}{c}\left[\frac{\partial}{\partial t}w_b-\frac{\partial}{\partial t}w_t\right]-\frac{c}{2}\frac{\partial\tau}{\partial x}\right)b$$
$$-m_b\frac{\partial^2}{\partial t^2}w_b+\frac{m_c d_b}{12}\frac{\partial^3}{\partial t^2\partial x}u_{0t}+\frac{m_c d_b}{6}\frac{\partial^3}{\partial t^2\partial x}u_{0b}+\frac{m_c d_b^2}{12}\frac{\partial^3}{\partial t^2\partial x}w_b-\frac{m_c d_b d_t}{24}\frac{\partial^3}{\partial t^2\partial x}w_t$$
$$-m_{1b}\frac{\partial^3}{\partial t^2\partial x}u_{0b}+m_{2b}\frac{\partial^4}{\partial t^2\partial x^2}w_b-\frac{m_c}{6}\frac{\partial^2}{\partial t^2}w_t-\frac{m_c}{3}\frac{\partial^2}{\partial t^2}w_b-+kg_1\cos^2(\theta)\frac{\partial^2}{\partial x^2}w_b \tag{26}$$
$$+kg_2\sin^2(\theta)\frac{\partial^2}{\partial x^2}w_b-k_w w_b-\mu\frac{\partial^2}{\partial x^2}\left[\frac{bd_b}{2}\frac{\partial\tau}{\partial x}+\frac{c}{2}\frac{\partial\tau}{\partial x}b-\frac{E_c b(w_b-w_t)}{c}-\frac{E_c g}{c}\left[\frac{\partial}{\partial t}w_b-\frac{\partial}{\partial t}w_t\right]\right.$$
$$-m_b\frac{\partial^2}{\partial t^2}w_b+\frac{m_c d_b}{12}\frac{\partial^3}{\partial t^2\partial x}u_{0t}+\frac{m_c d_b}{6}\frac{\partial^3}{\partial t^2\partial x}u_{0b}+\frac{m_c d_b^2}{12}\frac{\partial^3}{\partial t^2\partial x}w_b-\frac{m_c d_b d_t}{24}\frac{\partial^3}{\partial t^2\partial x}w_t-m_{1b}\frac{\partial^3}{\partial t^2\partial x}u_{0b}$$
$$\left.+m_{2b}\frac{\partial^4}{\partial t^2\partial x^2}w_b-\frac{m_c}{6}\frac{\partial^2}{\partial t^2}w_t-\frac{m_c}{3}\frac{\partial^2}{\partial t^2}w_b-+kg_1\cos^2(\theta)\frac{\partial^2}{\partial x^2}w_b+kg_2\sin^2(\theta)\frac{\partial^2}{\partial x^2}w_b-k_w w_b\right]=0,$$

$$u_{0t}b-u_{0b}b-\frac{b(c-d_t)}{2}\frac{\partial w_t}{\partial x}-\frac{b(c-d_b)}{2}\frac{\partial w_b}{\partial x}-\frac{bc^3}{12E_c}\frac{\partial^2\tau}{\partial x^2}+\frac{\tau bc}{G_c}$$
$$-k\frac{\partial^2}{\partial x^2}\left[-\frac{bc^3}{12E_c}\frac{\partial^2\tau}{\partial x^2}+\frac{\tau bc}{G_c}+u_{0t}b-u_{0b}b-\frac{b(c-d_t)}{2}\frac{\partial w_t}{\partial x}-\frac{b(c-d_b)}{2}\frac{\partial w_b}{\partial x}\right]=0. \tag{27}$$

3. Solution method

Based on Navier method, the displacements of the nano sandwich beam with simply supported boundary condition can be written as:

$$u_{0t}(x,t)=U_t.\cos\left(\frac{n.\pi.x}{l}\right).e^{\omega.t}, \tag{28}$$
$$u_{0b}(x,t)=U_b.\cos\left(\frac{n.\pi.x}{l}\right).e^{\omega.t}, \tag{29}$$
$$w_b(x,t)=W_b.\sin\left(\frac{n.\pi.x}{l}\right).e^{\omega.t}, \tag{30}$$
$$w_t(x,t)=W_t.\sin\left(\frac{n.\pi.x}{l}\right).e^{\omega.t}, \tag{31}$$
$$T(x,t)=T_0.\cos\left(\frac{n.\pi.x}{l}\right).e^{\omega.t}, \tag{32}$$

where n is vibration mode number and ω is frequency. Substituting Eqs. (28) - (32) into Eqs. (23) - (27), the motion equations in matrix form can be expressed as:

$$\begin{bmatrix} m_{11} & m_{12} & m_{13} & m_{14} & m_{15} \\ m_{21} & m_{22} & m_{23} & m_{24} & m_{25} \\ m_{31} & m_{32} & m_{33} & m_{34} & m_{35} \\ m_{41} & m_{42} & m_{43} & m_{44} & m_{45} \\ m_{51} & m_{52} & m_{53} & m_{54} & m_{55} \end{bmatrix} \ddot{X} + \begin{bmatrix} c_{11} & c_{12} & c_{13} & c_{14} & c_{15} \\ c_{21} & c_{22} & c_{23} & c_{24} & c_{25} \\ c_{31} & c_{32} & c_{33} & c_{34} & c_{35} \\ c_{41} & c_{42} & c_{43} & c_{44} & c_{45} \\ c_{51} & c_{52} & c_{53} & c_{54} & c_{55} \end{bmatrix} \dot{X} + \begin{bmatrix} k_{11} & k_{12} & k_{13} & k_{14} & k_{15} \\ k_{21} & k_{22} & k_{23} & k_{24} & k_{25} \\ k_{31} & k_{32} & k_{33} & k_{34} & k_{35} \\ k_{41} & k_{42} & k_{43} & k_{44} & k_{45} \\ k_{51} & k_{52} & k_{53} & k_{54} & k_{55} \end{bmatrix} X = 0, \tag{33}$$

where $X = \{U_t, U_b, W_t, W_b, T_0\}$ is dynamic vector, $\left[m_{ij} \right]$ is mass matrix, $\left[c_{ij} \right]$ is damper matrix and $\left[k_{ij} \right]$ is stiffness matrix, which are expressed in Appendix A. For the solution of final equations, the eigenvalue problem is used as:

$$\begin{aligned} &\left[\dot{X} \right] = [A][X], \\ &[A] = \begin{bmatrix} [0] & [I] \\ -\left[m^{-1}k \right] & -\left[m^{-1}c \right] \end{bmatrix}. \end{aligned} \tag{34}$$

4. Numerical results and discussion

The nano sandwich beam, including orthotropic face sheets and flexible core with below mechanical properties and geometric parameter, is considered:
Length of the structure: $l = 91.44nm$, thickness of the core: $c = 1.27nm$, thickness of the face sheet: $d_t = d_b = 0.045nm$, width of the face sheet: $b = 2.54nm$, elastic modulus of core: $E_c = 201.47Mpa$, core shear modulus: $G_c = 82.67Mpa$, density for core, top and bottom face sheets respectively: $\rho_c = 32.8, \rho_t = \rho_b = 2680\, kg/m^2$, elastic modulus for the top and bottom face sheets: $E_t = E_b = 6980Mpa$, Poisson's ratio of top and bottom face sheets: $\upsilon_t = \upsilon_b = 0.25$, parameter of size effect: $\mu = 1nm^2$, structure damping coefficient: $g = 1e^{-12}$, shear modulus of elastic medium: $kg_1 = kg_2 = 1e^{-10}$, spring constant of elastic medium: $kw = 1e^7$ and shear angle: $\theta = \pi / 4$.

4.1. Validation

For validating, the structural frequency of the sandwich beam without considering viscoelastic parameters, size effect and Pasternak orthotropic medium is compared with Refs. [12, 29]. Therefore, the frequencies of sandwich nano beam for five vibration modes are calculated and shown in Table 1 considering the mechanical properties and geometrical parameters the same as the Ref. [12, 29]. As can be seen, the results are in good agreement with those of Refs. [12, 29] , indicating the validation of this work.

Table 1. Comparison of frequencies of sandwich beam with Refs [12] and [29].

Frequencies (Hz)	Present model	Ref [12]	Ref [29]
Mode 1	250.7717	263	251
Mode 2	534.3375	-	537
Mode 3	866.5572	889	874
Mode 4	1265.4	1289	1282
Mode 5	1742.5	1774	1771

4.2. Effect of different parameters

Figures 2 and 3 show the effect of different thicknesses of top and bottom faces and structural damping on the natural frequency versus thickness of the core, respectively. It can be concluded that with an increase in the thickness, the frequency is increased as the stiffness of system is increased.

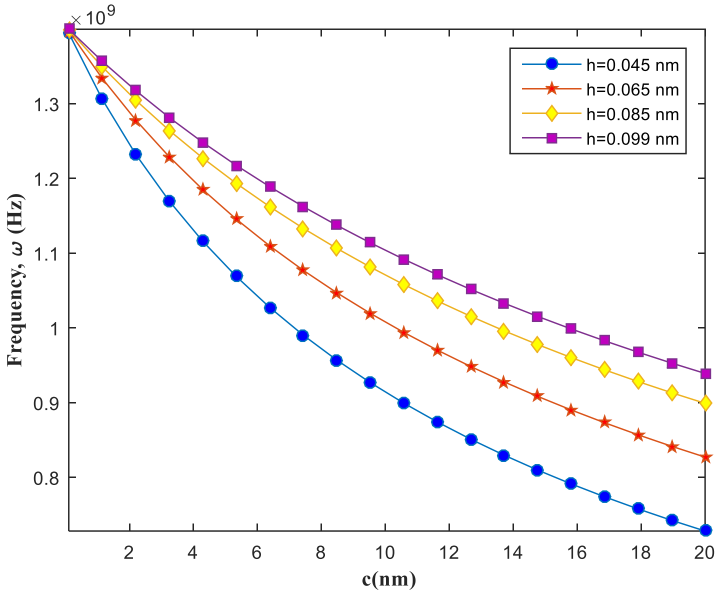

Fig. 2. Frequency versus thickness of core for different thickness of faces.

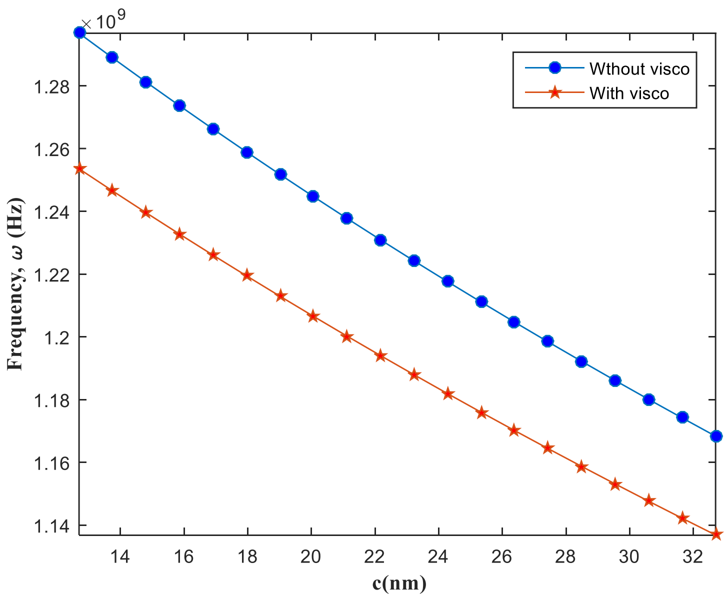

Fig. 3. Effect of viscoelastic parameter on the frequency versus thickness of core.

In addition, it can be seen that as the thickness of the core increases, the frequency decreases. The reason is that as the core thickness increases, the total stiffness of the structure is decreased. The study of viscous parameter shows that considering viscosity, the frequency of system is decreased. From Fig. 3, it can be seen that in the case in which the structural damping is considered, the frequency decreases up to 5.1% in comparison to the case in which the structural damping is not taken into account. The reason is that by increasing structural damping, the energy dissipation of the structure will be increased.

Figure 4 indicates the effect of spring constant of elastic medium on the frequency with respect to the thickness of the core. It is observed that by increasing spring constant of elastic medium, the frequency is increased. As can be observed, when the spring constant of elastic medium increases from $0.01e^{17}$ to $0.02e^{17}$, the frequency of the structure increases about 18.5%. The reason is because the stiffness of the system is increased by enhancing spring constant of elastic medium.

Figure 5 shows the study of size effect on the frequency with respect to the thickness of the core. It can be seen that by increasing the size effect, the frequency is reduced. The reason is that by enhancing size parameter, the bond length of the structure increases, leading to reduction in the stiffness of system. In addition, with an increase in the core thickness, the frequency is reduced. The reason is because the stiffness of core is lower than faces so enhancing its thickness, reducing the total stiffness of nano sandwich structure.

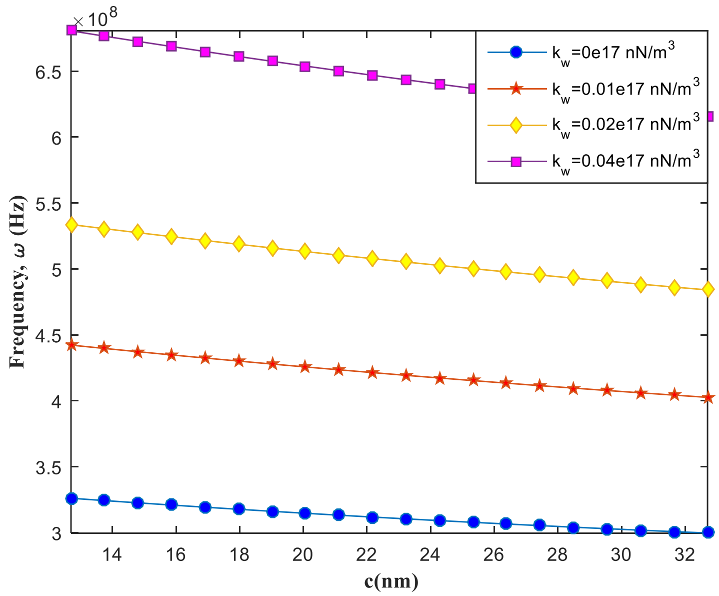

Fig. 4. Effect of spring constant of elastic medium on the frequency versus thickness of core.

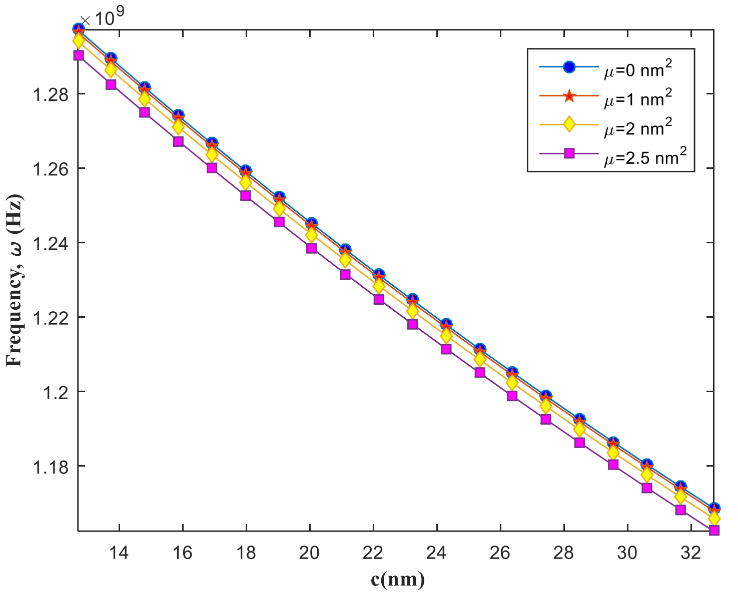

Fig. 5. Study of the size effect on the frequency versus thickness of core.

The frequency versus structural damping for different thicknesses of faces and core are shown in Fig. 6 and Fig. 7, respectively. It is found that when the thickness of faces increases from $0.045nm$ to $0.046nm$, the frequency of the structure increases by 0.152%. It can be concluded that by increasing the thickness of faces and decreasing the thickness of core, the frequency of system is increased. The reason is that by increasing the thickness of faces, the stiffness of the structure is increased.

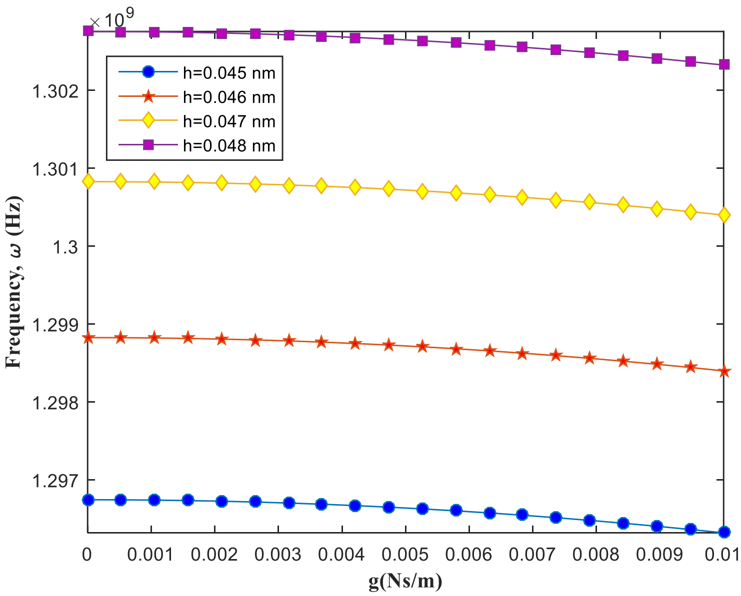

Fig. 6. Effect of thickness of faces on the frequency versus structural damping.

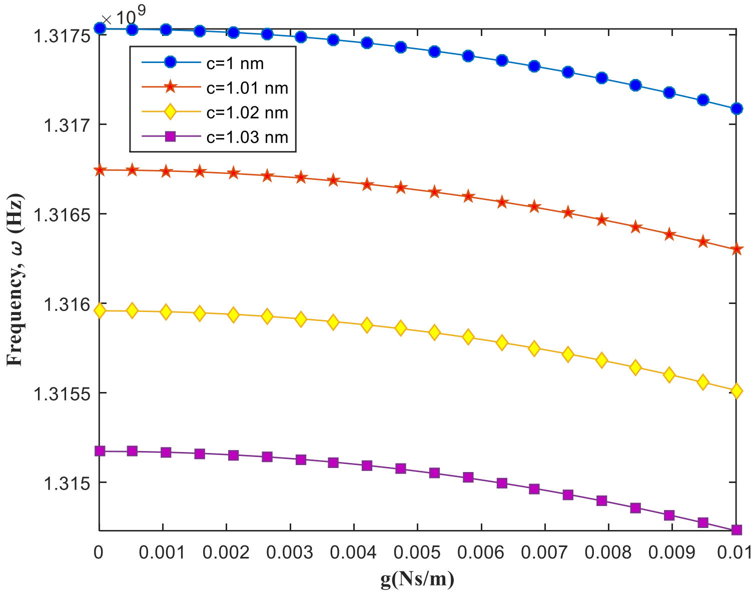

Fig. 7. Effect of thickness of flexible core on the frequency versus structural damping.

The study of size effect on the frequency versus structural damping is shown in Fig. 8. It is found that by increasing the size effect, the frequency is reduced due to decreasing the bending rigidity of the sandwich nano structure. Figure 9 indicates the effect shear modulus of elastic medium on the frequency respect to the spring constant of elastic medium. It is observed that by increasing shear and spring constants of elastic medium, the frequency is increased. For example, when the shear modulus of elastic medium increases from $0.2 nN/m$ to $0.3 nN/m$, the frequency of the structure increases up to 28.6 percent. Figures 10 and 11 shows the effect of spring constant and shear modulus of elastic medium on the frequency with respect to the length beam, respectively. It is observed that by increasing shear modulus and spring constant of the elastic medium, the frequency is increased which can be attributed to the increased stiffness of the system. It is also observed that by increasing the length beam, the frequency of system is decreased.

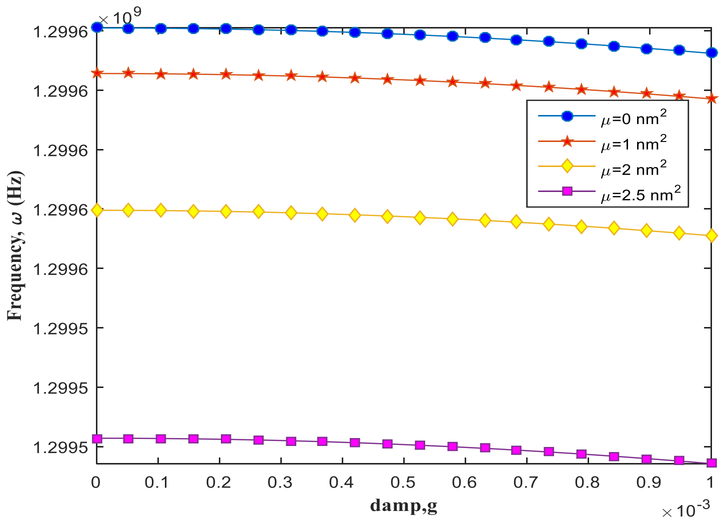

Fig. 8. Study of size effect on the frequency versus structural damping.

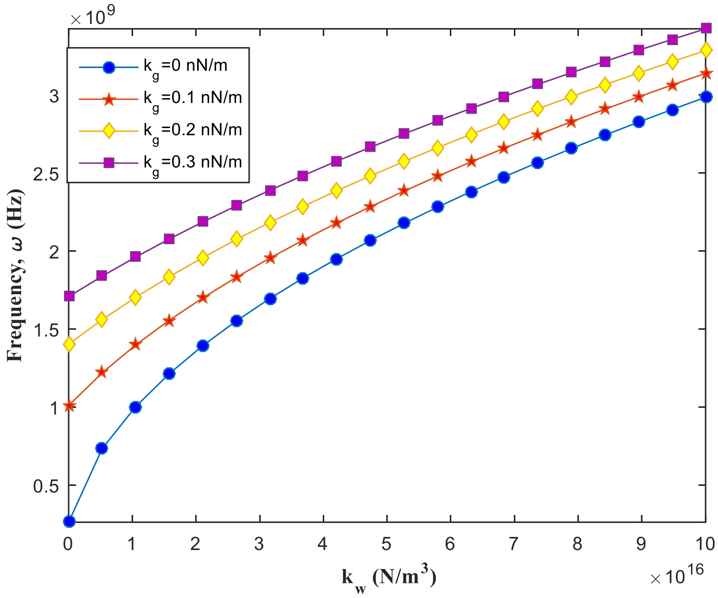

Fig. 9. Effect of shear modulus of elastic medium on the frequency versus spring constant of elastic medium.

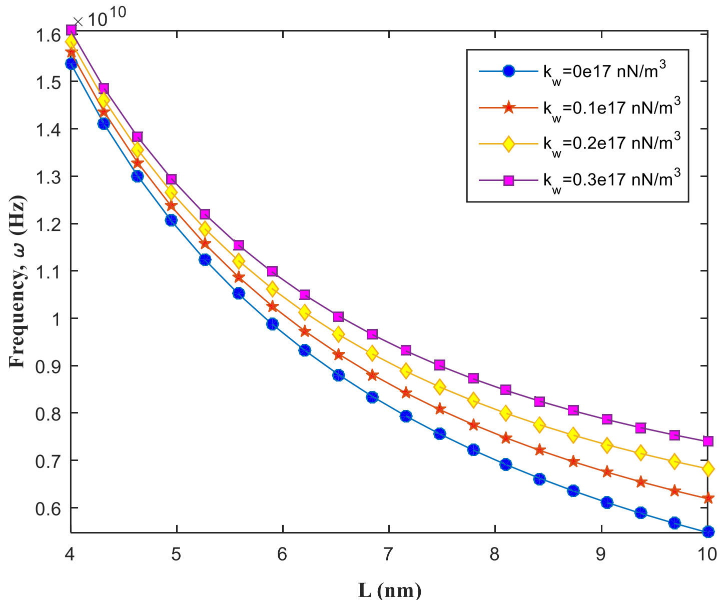

Fig. 10. Effect of spring modulus of elastic medium on the frequency versus beam length.

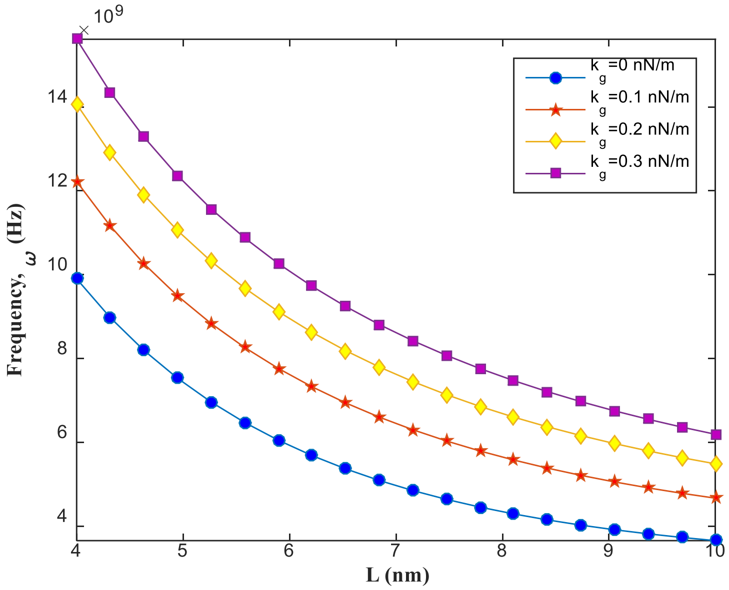

Fig. 11. Effect of shear constant of elastic medium on the frequency versus beam length.

The mode shapes for the first, second and third modes are shown in Fig. 12. As can be seen, the simply supported boundary conditions are satisfied in this figure.

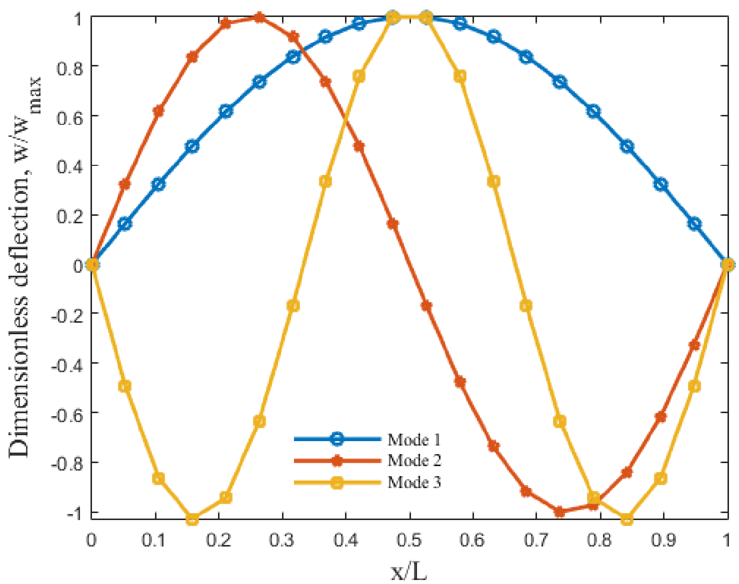

Fig. 12. Mode shapes of the sandwich nano beam.

5. Conclusion

In this research, vibration analysis of nano-sandwich beam was studied by considering the flexibility of the core. In the formulation, normal and shear stresses are considered for modeling the flexibility of the core. In this paper the sandwich beam was studied at nano-scale. In this regard, the high order sandwich panel theory was extended. The material properties of system were assumed viscoelastic using Kelvin–Voigt model. The elastic medium was simulated by orthotropic Pasternak medium. The Navier method was employed in order to obtain the natural frequency response of nano sandwich beam. The most findings of this paper are as follows: An increase in the size effect of sandwich beam leads to a reduction in the frequency. As the spring constant of elastic medium increases, the frequency is increased. By increasing the thickness of faces, the frequency is increased. By increasing the thickness of flexible core, frequency is decreased. Considering the viscos parameter, the frequency of sandwich beam is decreased.

Appendix A

$$m_{11}=-m_t-(\frac{1}{3})m_c-k\left[\frac{m_t n^2\pi^2}{L^2}+\frac{m_c n^2\pi^2}{3L^2}\right], \tag{A1}$$

$$m_{12}=-(\frac{1}{6})m_c-(\frac{1}{6})\left(\frac{km_c n^2\pi^2}{L^2}\right), \tag{A2}$$

$$m_{13}=(\frac{1}{6})\left(\frac{m_c d_t n\pi 1^2}{L}\right)+\left(\frac{m_{1t} n\pi 1^2}{L}\right)-k$$
$$\left[-(\frac{1}{6})\left(\frac{m_c d_t n^3\pi^3 1^2}{L^3}\right)-\left(\frac{m_{1t} n^3\pi^3 1^2}{L^3}\right)\right], \tag{A3}$$

$$m_{14}=-\left[\frac{m_c d_b n\pi}{12L}\right]-\left[\frac{km_c d_b n^3\pi^3}{12L^3}\right], \tag{A4}$$

$$m_{15}=0 \tag{A5}$$

$$m_{21}=-(\frac{m_c}{6})-\left[\frac{km_c n^2\pi^2}{6L^2}\right], \tag{A6}$$

$$m_{21}=-m_b-\left(\frac{m_c}{3}\right)-k\left[\frac{m_b n^2\pi^2}{L^2}+\frac{m_c n^2\pi^2}{3L^2}\right], \tag{A7}$$

$$m_{23}=\left(\frac{m_c d_t n\pi}{12L}\right)+\left(\frac{km_c d_t n^3\pi^3}{12L^3}\right), \tag{A8}$$

$$m_{24}=-\left[\left(\frac{m_c d_b n\pi 1^2}{6L}\right)\right]+\left[\left(\frac{m_{1b} n\pi 1^2}{L}\right)\right]-$$
$$k\left[\left(\frac{m_c d_b n^3\pi^3 1^2}{6L^3}\right)-\left(\frac{-m_{1b} n^3\pi^3 1^2}{L^3}\right)\right], \tag{A9}$$

$$m_{25}=0, \tag{A10}$$

$$m_{31}=\left(\frac{m_c d_t n\pi 1^2}{6L}\right)+\left(\frac{m_{1b} n\pi 1^2}{L}\right)-$$
$$k\left[\left(-\frac{m_c d_t n^3\pi^3 1^2}{6L^3}\right)-\left(\frac{m_{1b} n^3\pi^3 1^2}{6L^3}\right)\right], \tag{A11}$$

$$m_{32}=\left(\frac{m_c d_b n\pi}{12L}\right)+\left(\frac{k m_c d_b n^3\pi^3}{12L^3}\right), \tag{A12}$$

$$m_{33}=-m_t-k\left(\frac{m_t n^2\pi^2}{L^2}\right)-\left(\frac{m_c d_t^{\,2} n^2\pi^2 1^2}{12L^2}\right)-\left(\frac{m_{2t} n^2\pi^2 1^2}{L^2}\right)-$$
$$k.\left(\frac{m_{2t} n^4\pi^4 1^2}{L^4}\right)-\left(\frac{m_c 1^2}{3}\right)-k.\left(\frac{m_c n^2\pi^2 1^2}{3L^2}\right), \tag{A13}$$

$$m_{34}=\left(\frac{m_c d_b d_t n^2\pi^2 1^2}{24L^2}\right)-\left(\frac{m_c 1^2}{6}\right)-k\left(\frac{m_c n^2\pi^2 1^2}{6L^2}\right), \tag{A14}$$

$$m_{35}=0, \tag{A15}$$

$$m_{14}=-\left(\frac{m_c d_b n\pi}{12L}\right)-\left(\frac{k m_c d_b n^3\pi^3}{12L^3}\right), \tag{A16}$$

$$m_{42}=-\left(\frac{m_c d_b n\pi}{6L}\right)-\left(\frac{k m_c d_b n^3\pi^3}{6L^3}\right)+\left(\frac{m_{1b} n\pi 1^2}{L}\right)-$$
$$k.\left(\frac{-m_{1b} n^3\pi^3 1^2}{L^3}\right), \tag{A17}$$

$$m_{43}=\left(\frac{m_c d_b d_t n^2\pi^2 1^2}{24L^2}\right)-\left(\frac{m_c 1^2}{6}\right)-k\left(\frac{m_c n^2\pi^2 1^2}{6L^2}\right), \tag{A18}$$

$$m_{44}=-m_b-k\left(\frac{m_b n^2\pi^2}{L^2}\right)-\left(\frac{m_c d_b^{\,2} n^2\pi^2 1^2}{12L^2}\right)-\left(\frac{m_{2b} n^2\pi^2 1^2}{L^2}\right)-$$
$$k\left(\frac{m_{2b} n^4\pi^4 1^2}{L^4}\right)-\left(\frac{m_c 1^2}{3}\right)-k.\left(\frac{m_c n^2\pi^2 1^2}{3L^2}\right), \tag{A19}$$

$$m_{45}=0, \tag{A20}$$

$$m_{51}=0, \tag{A21}$$

$$m_{52}=0, \tag{A22}$$

$$m_{53}=0, \tag{A23}$$

$$m_{54}=0, \tag{A24}$$

$$m_{55}=0. \tag{A25}$$

$$c_{11}=\left(-\frac{A_t Egn^2\pi^2}{L^2}\right), \tag{A26}$$

$$c_{12}=0, \tag{A27}$$

$$c_{13}=0, \tag{A28}$$

$$c_{14}=0, \tag{A29}$$

$$c_{15}=0, \tag{A30}$$

$$c_{21}=0, \tag{A31}$$

$$c_{22}=\left(-\frac{gn^2\pi^2 EA_b}{L^2}\right), \tag{A32}$$

$$c_{23}=0, \tag{A33}$$

$$c_{24}=0, \tag{A34}$$

$$c_{25}=0, \tag{A35}$$

$$c_{31}=0, \tag{A36}$$

$$c_{32}=0, \tag{A37}$$

$$c_{33}=-\left(\frac{Egn^4\pi^4 I_t}{L^4}\right)+\left(-\frac{E_c gb}{c}\right)-k\left(\frac{E_c gn^2\pi^2 b}{L^2 c}\right), \tag{A38}$$

$$c_{34}=\left(\frac{E_c gb}{c}\right)-k.\left(-\frac{E_c gn^2\pi^2 b}{L^2 c}\right), \tag{A39}$$

$$c_{35}=0, \tag{A40}$$

$$c_{41}=0, \tag{A41}$$

$$c_{42}=0, \tag{A42}$$

$$c_{43}=\left(\frac{E_c gb}{c}\right)+k\left(\frac{E_c gn^2\pi^2 b}{L^2 c}\right), \tag{A43}$$

$$c_{44}=-\left(\frac{Egn^4\pi^4 I_b}{L^4}\right)-\left(\frac{E_c gb}{c}\right)-\left(\frac{kE_c gn^2\pi^2 b}{L^2 c}\right), \tag{A44}$$

$$c_{45}=0, \tag{A45}$$

$$c_{51}=0, \tag{A46}$$

$$c_{52}=0, \tag{A47}$$

$$c_{53}=0, \tag{A48}$$

$$c_{54}=0, \tag{A49}$$

$$c_{55}=0. \tag{A50}$$

$$k_{11}=-\left(\frac{n^2\pi^2 A_t E}{L^2}\right), \tag{A51}$$

$$k_{12}=0, \tag{A52}$$

$$k_{13}=0, \tag{A53}$$

$$k_{14}=0, \tag{A54}$$

$$k_{15}=b+kb\left(\frac{n\pi}{L}\right)^2, \tag{A55}$$

$$k_{21}=0, \tag{A56}$$

$$k_{22}=-\left(\frac{n^2\pi^2 EA_b}{L^2}\right), \tag{A57}$$

$$k_{23}=0, \tag{A58}$$

$$k_{24}=0, \tag{A59}$$

$$k_{25}=-b-kb\left(\frac{n\pi}{L}\right)^2, \tag{A60}$$

$$k_{31}=0, \tag{A61}$$

$$k_{32}=0, \tag{A62}$$

$$k_{33}=-\left(\frac{En^4\pi^4 I_t}{L^4}\right)+\left(-\frac{E_c 1b}{c}\right)-k\left(\frac{E_c n^2\pi^2 b}{L^2 c}\right), \tag{A63}$$

$$k_{34}=\left(\frac{E_c b}{c}\right)+\left(\frac{kE_c n^2\pi^2 b}{L^2 c}\right), \tag{A64}$$

$$k_{35}=-\left(\frac{n\pi bd_t}{2L}\right)-\left(\frac{Cn\pi b}{2L}\right)-k\left[\frac{n^3\pi^3 bd_t}{2L^3}+\frac{Cn^3\pi^3 b}{2L^3}\right], \tag{A65}$$

$$k_{41}=0, \tag{A66}$$

$$k_{42}=0, \tag{A67}$$

$$k_{43}=\left(\frac{E_c 1b}{c}\right)+k\left(\frac{E_c n^2\pi^2 b}{L^2 c}\right), \tag{A68}$$

$$k_{44}=-\left(\frac{En^4\pi^4 I_b}{L^4}\right)-\left(\frac{E_c b}{c}\right)-k\left(\frac{E_c n^2\pi^2 b}{L^2 c}\right)-kg_1\left[\frac{cos(\theta)^2 n^2\pi^2}{L^2}\right]- \tag{A69}$$

$$kg_2\left[\frac{sin(\theta)^2 n^2\pi^2}{L^2}\right]-K_w-$$

$$k\left(\frac{kg_1 cos(\theta)^2 n^4\pi^4}{L^4}+\frac{kg_2 sin(\theta)^2 n^4\pi^4+}{L^4}+\frac{K_w n^2\pi^2}{L^2}\right),$$

$$\mathrm{k}_{45}=-\left(\frac{\mathrm{n}\pi\mathrm{bd}_{\mathrm{b}}}{2L}\right)-\left(\frac{\mathrm{Cn}\pi\mathrm{b}}{2L}\right)-k\left(\frac{n^3\pi^3bd_b}{2L^3}+\frac{Cn^3\pi^3b}{2L^3}\right), \tag{A70}$$

$$\mathrm{k}_{51}=\mathrm{b}, \tag{A71}$$

$$\mathrm{k}_{52}=-\mathrm{b}, \tag{A72}$$

$$k_{53}=-\left(\frac{n\pi b(c+d_t)}{2L}\right)-\left(\frac{kn^3\pi^3b(c+d_t)}{2L^3}\right), \tag{A73}$$

$$k_{54}=-\left(\frac{n\pi b(c+d_b)}{2L}\right)-\left(\frac{kn^3\pi^3b(c+d_b)}{2L^3}\right), \tag{A74}$$

$$k_{55}=\left(\frac{n^2\pi^2bc^3}{12(L^2E_c)}\right)+\frac{bc}{G_c}-k\left[-\left(\frac{n^4\pi^4bc^3}{12(L^4E_c)}\right)-\left(\frac{n^2\pi^2bc}{(G_cL^2)}\right)\right]. \tag{A75}$$

References

[1] Nayak, A.K., Moy, S.S.J., Shenoi, R.A., 2005. A higher order finite element theory for buckling and vibration analysis of initially stressed composite sandwich plates. Journal Sound and Vibration. 286, 763–780.

[2] AhmerWadee, M., Yiatros, S., Theofanous, M., 2010. Comparative studies of localized buckling in sandwich struts with different core bending models. International Journal of Non-Linear Mechanics. 45, 111–120.

[3] ElMeiche, N., Tounsi, A., Ziane, N., Mechab, I., El Bedia, A.A., 2011. A new hyperbolic shear deformation theory for buckling and vibration of functionally graded sandwich plate. International Journal of Mechanical Science. 53, 237–247.

[4] Rohlfing, J., Gardonio, P., Thompson, D.J., 2011. Comparison of decentralized velocity feedback control for thin homogeneous and stiff sandwich panels using electrodynamic proof-mass actuators. Journal Sound and Vibration. 330, 843–867.

[5] Ghayesh, M.H., 2011. Nonlinear forced dynamics of an axially moving viscoelastic beam with an internal resonance. International Journal of Mechanical Science. 53, 1022–1037.

[6] Liu, D., Wei, X., Yong, X. 2012. Dynamic responses of axially moving viscoelastic beam under a randomly disordered periodic excitation. Journal Sound and Vibration. 331, 4045–4056.

[7] Ghayesh, M. H., Amabili, M., 2012. Nonlinear dynamics of axially moving viscoelastic beams over the buckled state. Computers & Structures, 112–113, 406–421

[8] Azoti, W.L., Koutsawa, Y., Bonfoh, N., Lipinski, P., Belouettar, S., 2013. Analytical modeling of multilayered dynamic sandwich composites embedded with auxetic layers. Engineering Structures. 57, 248–253.

[9] Laine, C., Grognec, P., ComasCardona, S.b., Binetruy, C., 2013. Analytical, numerical and experimental study of the bifurcation and collapse behavior of a 3D reinforced sandwich structure under through- thickness compression. International Journal of Mechanical Science. 67, 42–52

[10] Kueh, A. B. H., 2013. Buckling of sandwich columns reinforced by triaxial weave fabric composite skin-sheets. International Journal of Mechanical Science. 66, 45–54.

[11] Teodor, M., Atanackovic, B., Pilipovic, S., Zorica, D., 2013. Forced oscillations of a body attached to a viscoelastic rod of fractional derivative type. International Journal of Engineering Science. 64, 54–65.

[12] Khalili, S.M.R., Botshekanan Dehkordi, M., Carrera, E., Shariyat, M., 2013. Non-linear dynamic analysis of a sandwich beam with pseudoelastic SMA hybrid composite faces based on higher order finite element theory. Composite Structures. 96, 243–255.

[13] El Mir, C., Toubia, E., Brockman, R., 2014. Analysis of cylindrical sandwich structures with weak orthotropic core under patch loading. Engineering Structures. 80, 89–97.

[14] Nayak, B., Dwivedy, S.K., Murthy, K.S.R.K., 2014. Dynamic stability of a rotating sandwich beam with magnetorheological elastomer core. European Journal of Mechanics; A/Solids. 47, 143-155.

[15] Magnucka-Blandzi, E., 2018. Bending and buckling of a metal seven-layer beam with crosswise corrugated main core – Comparative analysis with sandwich beam. Composite Structures. 183, 35-41.

[16] Krysko, A.V., Awrejcewicz, J., Kutepov, I.E., Krysko, V.A., 2017. Stability of curvilinear Euler-bernoulli beams in temperature. International Journal of Non-Linear Mechanics. 94, 207-215.

[17] Komijani, M., Gracie, R., 2016. Nonlinear thermo-electro-mechanical dynamic behaviour of FGPM Beams. Composite Structures. 150, 208–218.

[18] Xiaobai, Li., Li, L., Yujin, Hu., Zhe, D., Weiming, D., 2017. Bending, buckling and vibration of axially functionally graded beams based on nonlocal strain gradient theory. Composite Structures. 165, 250–265.

[19] Chen, L.Q., Tang, Y.Q., Lim, C.W., 2010. Dynamic stability in parametric resonance of axially accelerating viscoelastic Timoshenko beams. Journal of Sound and Vibration. 329, 547–565.
[20] Ghiasian, S.E., Kiani, Y., Eslami, M.R., 2013. Dynamic buckling of suddenly heated or compressed FGM beams resting on nonlinear elastic foundation. Composite Structures. 106, 225–234.
[21] Lei, Y., Adhikari, S., Friswell, M.I., 2013. Vibration of nonlocal Kelvin–Voigt viscoelastic damped Timoshenko beams. International Journal of Engineering Science. 66, 1–13.
[22] Eltaher, M.A., Khairy, A., Sadoun, A.M., Alzahraa, O.F., 2014. Static and buckling analysis of functionally graded Timoshenko Nanobeams. Applied Mathematics and Computation, 229, 283–295.
[23] Ilkhani, M.R., Hosseini-Hashemi, S.H., 2016. Size dependent vibro-buckling of rotating beam based on modified couple stress theory. Composite Structures. 143, 75–83.
[24] Shojaeian, M., Zeighampour, H., 2016. Size dependent pull-in behavior of functionally graded sandwich nanobridges using higher order shear deformation theory. Composite Structures. 143, 117–129.
[25] Kolahchi, R., 2017. A comparative study on the bending, vibration and buckling of viscoelastic sandwich nanoplates based on different nonlocal theories using DC, HDQ and DQ methods. Aerospace Science and Technology. 66, 235-248.
[26] Tang, Y., Liu, Y. and Zhao, D. 2017. Effects of neutral surface deviation on nonlinear resonance of embedded temperature-dependent functionally graded nanobeams, 2017, Composite Structures. 184, 23-33.
[27] Arefia, M., Zenkourb, A.M. 2017. Thermo-electro-magneto-mechanical bending behavior ofsize-dependent sandwich piezomagnetic nanoplates. Mechanics Research Communications. 84, 27–42.
[28] Li, Y.H, Donga, Y.H., Qina, Y., Lv, H.W. 2018. Nonlinear forced vibration and stability of an axially moving viscoelastic sandwich. International Journal of Mechanical Sciences. 138, 131-145.
[29] Frostig, Y., Baruch, M. 1994. Free vibration of sandwich beams with a transversely flexible core: a high order approach. Journal of Sound and Vibration. 176(2), 195-208.